

Development of a High-Power Monotron for RF Applications in Spherical Tokamaks

J. J. Barroso, K. G. Kostov, P. J. Castro, J. O. Rossi, H. Patire, Jr., G. O. Ludwig, J. A. Gonçalves, G. M. Sandonato, and J. P. Leite Neto

Associated Plasma Laboratory, INPE, P.O. Box 515, São José dos Campos, SP, Brazil

Abstract: Electron cyclotron heating (ECH) assist has been demonstrated to significantly improve startup performance of tokamaks by decreasing the loop voltage, which translates into ramp current rates higher than those of pure Ohmic startup at equivalent loop voltages. This has been observed on several machines that normally rely on the use of gyrotrons or an assembly of klystrons to produce such beneficial effects at particular electron cyclotron resonance frequencies. However, specific RF source requirements in terms of frequency and power demand specially customized designs, leading to costly industrial tubes. In light of these considerations, pre-ionization and plasma production on the ETE spherical tokamak of LAP/INPE are currently being pursued on the basis of the monotron, which, consisting of an electron beam that traverses a standing-wave cavity resonator, ranks as the simplest microwave tube. Thus describing the design, construction techniques and simulation results of a high-power microwave tube, the present paper reports on a proof-of-principle monotron experiment currently under way at our laboratory.

1. Introduction

Having been known since the 1930s [1,2], the monotron is a transit-time oscillator where the beam electrons cross the interaction space in a transit angle close to $(4k+1)\pi/2$ where k is an integer. Under this synchronism condition, the beam can interact unstably with a cavity mode, causing the RF field to grow at the expense of the DC beam energy [3,4]. Electron bunches are formed in the beam and reach the cavity end plate in a decelerating phase of the RF field thus transferring energy to the cavity RF field. The bunches constitute a fluctuating component of the convection current that induces in the resonator walls an RF current to sustain the oscillations. The present paper addresses the monotron by examining its capabilities regarding high efficiency operation with three hollow concentric beams to produce hundreds of kilowatt power output.

2. High-Efficiency Operating Regime

The analysis developed in this section is a one-dimensional Lagrangian treatment in which a representative number of electrons injected at the input plane is traced through the cavity taking account of the presence of a standing-wave electric field. Neglecting the space-charge forces between the charged particles in the beam, the normalized force equation is written as

$$\frac{d\tilde{p}}{d\tilde{t}} = \left[\frac{A}{\tilde{d}} \frac{\varepsilon_0}{mc^2} \right] \cos(\tilde{t} + \varphi) \cos(l\pi\tilde{z}/\tilde{d}) \quad (1)$$

with

$$\frac{d\tilde{z}}{d\tilde{t}} = \frac{\tilde{p}(t)c}{\sqrt{m^2c^2 + \tilde{p}^2}} \quad (2)$$

where $\tilde{p} = p(t)/mc$ is the normalized electron momentum, with the time normalized as $\tilde{t} = 2\pi t/T$ and the distance as $\tilde{z} = z\omega/c$, $q = -e$ and m are the electronic charge and the electron rest mass, φ specifies the electron entrance phase, l is an integer number defining the field distribution along the normalized interaction length $\tilde{d} = d\omega/c$; $\varepsilon_0 = qV_0$ denotes the initial energy of the injected beam, where V_0 is beam voltage; $A = V/V_0$ is defined as the field amplitude parameter where $V = E/d$ is the maximum RF voltage established across the cavity.

Given an axial number l and specifying the initial electron momentum, we infer that the final momentum of a single electron upon reaching the collector plate at $z=d$ on a transit time $\tau(\varphi)$ is determined by the entrance phase φ and by the set of parameters \tilde{d} , A , and ε_0 . The corresponding final kinetic energy for a single electron is

$$\varepsilon_s(\tau) = mc^2 \left(\sqrt{1 + (p(\tau)/mc)^2} - 1 \right) \quad (3)$$

and the kinetic energy of the exit beam at $z=d$ is calculated by averaging out the individual electron energies over the phase φ

$$\langle \varepsilon_B \rangle = \frac{1}{2\pi} \int_0^{2\pi} \varepsilon_s(\tau) d\varphi = \frac{1}{N} \sum_{k=1}^N \varepsilon_{k,s}(d) \quad (4)$$

where N is the total number of electrons injected during a period T . The electronic efficiency is expressed by $\eta_{el} = 1 - \langle \varepsilon_B \rangle / \varepsilon_0$. On account of (1) the efficiency is seen to be a function of the normalized quantities A , \tilde{d} , and ε_0 , i.e. $\eta_{el} = \eta_{el}(A, \tilde{d}, \varepsilon_0)$ for a given index l specifying the electric field axial profile. If η_{el} thus calculated is positive, then the electrons transfer energy to the RF field. In what follows, the electronic efficiency is maximized and given as a function of the single parameter \tilde{d} . The input beam energy ε_0 and the axial number l are fixed and (1) is numerically integrated using the optimum value of the amplitude parameter A such that a maximum efficiency is calculated from (4) with $N=500$.

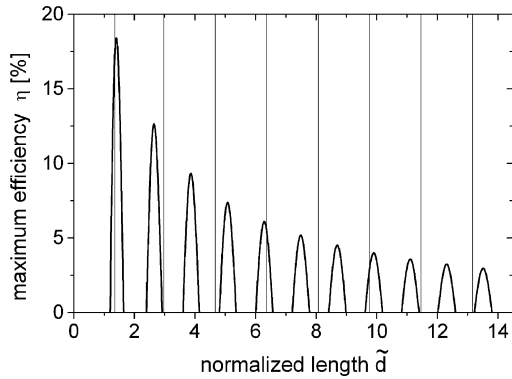


Fig. 1. Maximum electronic efficiency vs normalized length \tilde{d} for $l=0$, $\varepsilon_0=10\text{keV}$, and $A=3.9$.

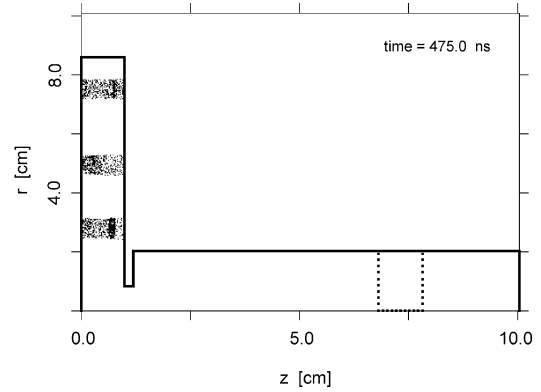


Fig. 2 Simulation configuration of the triple-beam monotron, showing bunched beams.

Considering $\varepsilon_0 = 10\text{keV}$ and $l=0$ modes, a typical tuning curve is shown in Fig.1. This figure brings a discrete set of beam modes with $\eta_{el,\text{max}}$ peaking at evenly spaced values of \tilde{d} i.e., $\tilde{d}_{\text{max}} = 1.4, 2.6, 3.8, \dots$. For comparison purposes, the vertical lines dropping to the \tilde{d} -axis in Fig. 1 indicate the resonant frequencies of the TM_{0n0} , $n=1,2,3,\dots,11$ modes in a circular cylindrical cavity of length $d=1.0$ cm and radius $R_w=1.85$ cm.

The maximum efficiency, at $\varepsilon_0=10\text{keV}$, reaches 18.5% for operation in $l=0$ modes at $\tilde{d}=1.4$ as illustrated by Fig. 1. In this condition, the optimum DC electron transit time τ_0 has been found to be $\tau_0 \approx (n+0.15)T$ with $n=1,2,\dots,11$ corresponding to the beam modes in Fig. 1. It is seen that the cavity parameter $\tilde{d}=1.3$ corresponding to the resonating TM_{010} mode ($n=1$) in the test cavity is somewhat less than the optimum $\tilde{d}=1.4$ required by the 10-keV electron beam, since the vertical frequency line passes on the left of the highest efficiency peak at $\tilde{d}=1.4$. Instead of lowering ε_0 , which is equivalent to shifting the whole beam spectrum to the left, an alternate approach to provide the optimum cavity-beam coupling is to increase the

cavity \tilde{d} from 1.3 to 1.4. Noting that $\tilde{d} = d\omega/c$ and that the cavity radius R_w is determined from the boundary condition, $R_w (cm) = (15/\pi)\chi_{0n}/f(GHz)$ one gets $R_w = \chi_{0n}d/\tilde{d}$ where χ_{0n} denotes the n -th zero of the Bessel function J_0 . Keeping constant the interaction length $d=1.0$ cm, and considering operation in the TM_{010} mode ($\chi_{01}=2.4048$), the cavity radius has to be decreased from 1.85 cm to 1.72 cm for optimum operation. Selecting, however, the higher order TM_{040} mode $\chi_{04}=11.7915$ the required cavity radius is calculated as $R_w=8.42$ cm.

3. Triple-Beam Monotron

This Section describes the nominal geometry of a monotron having three annular beams at the maxima of the radial distribution of the electric field in a TM_{040} -mode cavity with a circular aperture through which electromagnetic energy stored in the resonant cavity is extracted to the output guide. At an injection beam energy $\varepsilon_0 = 10keV$, the optimum cavity dimensions of the monotron considered here have been determined in the previous section as length $d=1.0$ cm and radius $R_w=8.42$ cm, which gives a resonant frequency $f = (15/\pi)(p_{04}/R_w(cm))=6.68$ GHz, and normalized length $\tilde{d} = 1.4$. By viewing the cavity as a short-circuited diode, the beams are injected from the left and run in the temperature-limited regime with each current in proportion to the area of the beams' cross-section, i.e., $I_i = J_c/\pi[r_{2,i}^2-r_{1,i}^2]$ where J_c is the current density. The beams are 0.4-cm thick and centered at the positions $r=2.8, 5.1,$ and 7.4 cm, which correspond to three consecutive maxima of the radial electric field distribution for the TM_{04} mode in an empty circular cavity. As depicted in Fig. 2, the resonant cavity is aperture coupled by means of a circular iris that transmits the RF power generated in the cavity to the 2.0-cm-radius output guide in which the lowest order TM_{01} mode propagates down. In the waveguide, a resistive disk is inserted having a resistance per unit square equal to the characteristic wave impedance of the TM_{01} output wave to absorb completely the incident wave[4].

4. PIC Code Simulation Results

By considering two values of R_i namely 0.8 cm and 0.9 cm in the monotron configuration of Fig. 2, the results given in this section encompass the overall efficiency η and average output power P_{out} over a total current range. The output power and total efficiency have been calculated from particle-in-cell (PIC) simulations. The program used is the KARAT code [5], that is based on 2 1/2-D axisymmetric PIC model in which the Maxwell's equations and the equation of motion for macroparticles are solved self-consistently. The physical system is run on a grid with square cells 1 mm size with over three thousand macroparticles representing each beam in the configuration space as shown in Fig. 2 during steady state when the electron beams become fully density-modulated.

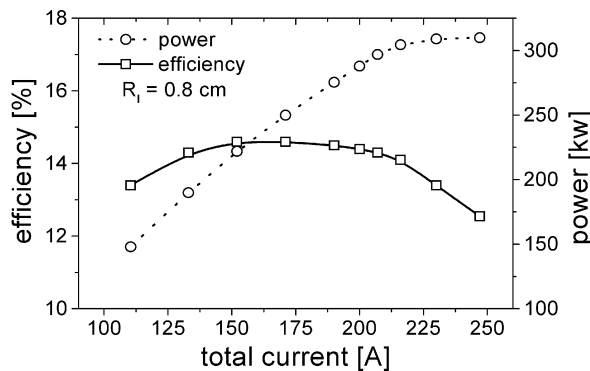


Fig. 3. Dependence of output power and overall efficiency on total current for $R_i=0.8$ cm.

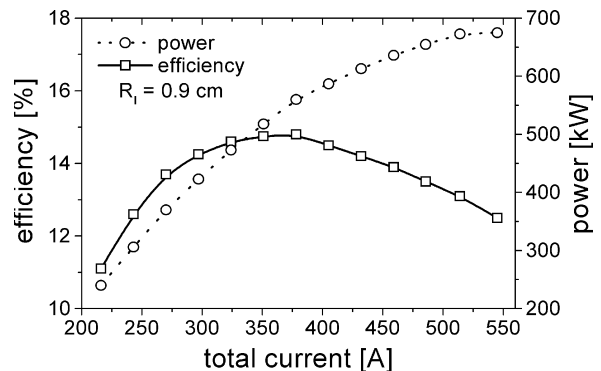


Fig. 4. Dependence of output power and overall efficiency on total current for $R_i=0.9$ cm.

For $R_1=0.8$ cm, the dependence of both P_{out} and η on total current is presented in Fig. 3. About the output power, it is seen in Fig. 3 that P_{out} closely follows a linear increase with current before saturating at 320 kW for current levels above 230 A; the corresponding efficiency curve features a flat region of 14.5% efficiencies. Similar plots of P_{out} and η for $R_1=0.9$ cm are given in Fig. 4. In this case, while saturating at 670 kW for currents in excess of 525 A, the output power reaches the optimal value of 560 kW at 14.8% efficiency and 378 A current.

For the higher power case discussed above, the total time history of output power at $z=5.0$ cm is shown in Fig. 5. On steady state the constant-amplitude signal corresponds to the average power level of 560 kW. It is to be noted that the waveform amplitude is always positive, meaning that the output signal is a positive traveling wave. The frequency spectrum of the steady state electric field at the point $z=5.0$ cm, $r=1.0$ cm in the output guide is shown in Fig. 6, with a sharp spectrum centered at 6.67GHz, very close to the cold cavity eigenfrequency of 6.68 GHz.

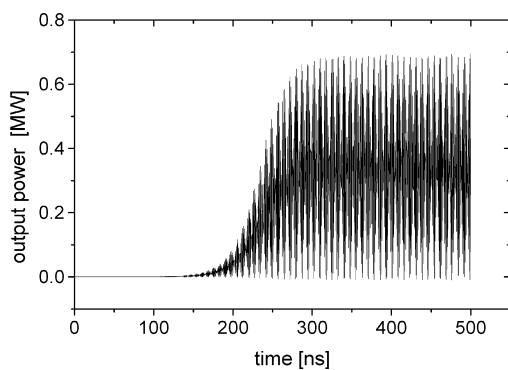


Fig. 5. Total time history of RF output power at section $z=5.0$ cm of the output guide.

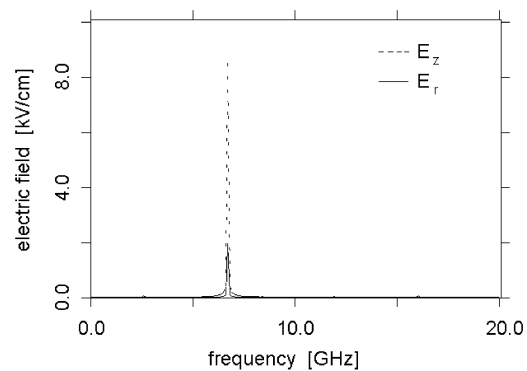


Fig. 6. Frequency spectrum of electric field at $r=1.0$ cm, $z=5.0$ cm.

5. Conclusions

A triple-beam TM_{040} monotron oscillator has been presented for which a 2 $1/2$ -D particle-in-cell simulation has indicated output powers in excess of 500 kW at 6.7GHz. The system includes a simple structure where the elementary functions of electron bunching and energy transfer to the RF field are performed in a single circular cylindrical cavity, which makes the monotron a compact, lightweight device. The cavity geometry (radius 8.42 cm, length 1.0 cm) and operating beam energy (10 keV) have been determined on the basis of a one-dimensional analysis, upon neglecting space-charge forces, that predicts a conversion efficiency of about 15.5%. The system has mechanical simplicity, and circular symmetry, for easy machining and assembly as well as a solid anode block for improved cooling and thermal management in long pulse operation. Such characteristics make the device practical from the viewpoint of cost and flexibility, allowing simple procedures for scaling power and frequency.

References

- [1] C. K. Birdsall, and W. B. Bridges, *Electron Dynamics of Diode Regions*, New York: Academic Press, 1966, sec. 1.06.
- [2] J. J. Müller and E. Rostas, "Un generateur a temps de transit utilisant un seul resonateur de volume", *Helvet. Phys. Acta*, vol. 13, pp. 435-450, Oct. 1940.
- [3] J. J. Barroso, and K. G. Kostov "A 5.7GHz, 100 kW microwave source based on the monotron concept", *IEEE Trans. Plasma Science*, vol. 27, pp. 580-586, April 1999.
- [4] J. J. Barroso, "Design facts in the axial monotron", *IEEE Trans. Plasma Science*, vol. 28, pp. 652-656, June 2000.
- [5] V. P. Tarakanov, "User's Manual for Code KARAT", Berkeley Research Associates., Inc., Springfield, USA, 1994.